

A globally applicable model of daily solar irradiance estimated from air temperature and precipitation data¹

Jerome C. Winslow^{a,2}, E. Raymond Hunt Jr^{a,*}, Stephen C. Piper^b

^a Department of Botany, University of Wyoming, Laramie, WY 82071-3165, USA

^b Scripps Institution of Oceanography, University of California San Diego, La Jolla, CA 92093-0220, USA

Received 24 March 2000; received in revised form 9 March 2001; accepted 27 March 2001

Abstract

Although not measured at many ground stations, the total daily solar irradiance (R_s) received at the earth's surface is a critical component of ecosystem carbon, water and energy processes. Methods of estimating R_s from other meteorological data, particularly daily temperatures, have not worked as well in tropical and maritime areas. At Luquillo, Puerto Rico, the daily atmospheric transmittance for solar radiation was approximately equal to one minus the daily-average relative humidity ($1 - rh_{ave}$). From these observations, we developed a model (VP-RAD) for estimation of R_s with inputs of daily maximum and minimum air temperature, daily total precipitation, mean annual temperature, mean annual temperature range, site latitude, and site elevation. VP-RAD performed well over large areas; it showed a good agreement with the site data used for model development and for seven other warm, humid locations in the southeastern United States. Comparisons with a similar model revealed that predictions using VP-RAD had lower average errors and improved day-to-day correlation to measured solar irradiance. In a global comparison for the year 1987, VP-RAD-estimated and satellite-derived photosynthetically active radiation converged to within $1.0 \text{ MJ m}^{-2} \text{ day}^{-1}$ at 72% of the 13072 1° latitude by 1° longitude vegetated grid cells. Although these comparisons revealed areas where VP-RAD may need improvement, VP-RAD should be a useful tool for applications globally. In addition, VP-RAD's similarity in form to the Bristow–Campbell equation provides a convenient method to calculate the site-specific coefficients for this model that is widely used when solar irradiance data are not available. © 2001 Elsevier Science B.V. All rights reserved.

Keywords: Solar irradiance; Atmospheric transmittance; Relative humidity; Atmospheric vapor pressure; Daily temperature range; Photosynthetically active radiation; Bristow–Campbell equation

* Corresponding author. Present address: Hydrology and Remote Sensing Laboratory, BARC-West, Building 007, Room 104, USDA Agricultural Research Service, 10300 Baltimore Avenue, Beltsville, MD 20705-2350, USA. Tel.: +1-301-504-5278; fax: +1-301-504-8931.

E-mail address: erhunt@hydrolab.arsusda.gov (E.R. Hunt, Jr).

¹ Texas Tech University College of Agricultural Sciences and Natural Resources Manuscript Number T-9-901.

² Present address: Department of Range, Wildlife and Fisheries Management, Texas Tech University, Lubbock, TX 79409 USA, and USDA Agricultural Research Service Plant Stress and Water Conservation Laboratory, Lubbock, TX 79415 USA.

1. Introduction

1.1. Background

The daily solar irradiance at the earth's surface (R_s , MJ m⁻² day⁻¹) is a fundamental driving variable for simulation of ecosystem carbon, water, and energy fluxes at local, regional, and global scales. However, R_s is seldom measured and lacking at most locations where models are applied. R_s may be determined from satellites (Pinker and Laszlo, 1992; Gu and Smith, 1997), cloud cover, or from global climate models, although either the spatial resolution or the temporal resolution is inadequate for site-specific analyses that include variations in topography. Stochastic weather generators are able to generate daily simulations from data averages (Friend, 1998), and monthly-average solar irradiances can be estimated from other meteorological data (Nikolov and Zeller, 1992; Yin, 1996). However, data averages hide the specific sequence of cold-or-warm, wet-or-dry days that is an important factor in processes such as vegetation net primary production (Hunt et al., 1991).

1.2. Bristow and Campbell equation

Bristow and Campbell (1984) devised an empirical algorithm for estimating R_s from only daily maximum and minimum air temperatures (T_{\max} and T_{\min} , respectively, °C) and daily total precipitation (*prcp*, mm). Their model reduces the total daily solar radiation incident at the top of the atmosphere (Q_o , MJ m⁻² s⁻¹) by the fraction lost due to clouds so that

$$R_s = \tau Q_o \quad (1)$$

where τ is the daily total atmospheric transmittance to solar radiation. Formulae to calculate Q_o and R_s for different slopes, aspects, latitudes and times are found in Sellers (1965), Gates (1980), Nikolov and Zeller (1992), and Antonić (1998). Bristow and Campbell formulated a prediction equation for the transmittance:

$$\tau = A[1 - \exp(-B \cdot \Delta T^C)] \quad (2)$$

where A , B and C are empirical coefficients unique to each location, and ΔT is the difference between T_{\max} and T_{\min} corrected for temperature changes caused by horizontal warm or cold air advection.

The actual physical processes that occur in the lower atmospheric boundary layer cannot be described in sufficient detail (as of yet) to yield the simple equation described by Bristow and Campbell. However, certain elements of the equation can be given a physical definition. Because of the structure of the equation, coefficient A sets the upper limit of τ . Consequently, A can be regarded as the cloud-free transmissivity, and the exponential portion of the equation represents the daily reduction in transmissivity that occurs primarily because of cloud cover. Simple physical definitions for coefficients B and C are not possible, but Bristow and Campbell noted that B and C represent the local sensitivity of the daily temperature range to the total incoming radiation. This sensitivity depends upon the local partitioning of solar energy that varies with altitude and season. In addition, because of the structure of the regression, B and C are interrelated and estimation errors introduced by one of the coefficients force changes in the other.

The simplicity of the Bristow–Campbell equation and its predictive accuracy make it attractive for use in global ecosystem simulations. However, it was designed for use on a site-by-site basis with coefficients A , B , and C derived from long-term climatological data, a procedure that is impractical for analyses over large areas. Faced with no simple alternative, large regions are simulated using the Bristow–Campbell equation by assuming that coefficients B and C do not vary from place to place, and A varies with elevation only. Variations of this method are incorporated in the models MT-CLIM (Running et al., 1987) and RHESys (Running et al., 1989). This approach works surprisingly well in many geographical areas, but not in others; predictions are best at locations with continental climates. Goodness-of-fits (R^2) between predicted and observed radiation are about 0.7 (Glassy and Running, 1994; Thornton et al., 1997). However, Hunt et al. (1996) tried this method for a simulation of the global carbon

budget and found that radiation was underestimated significantly in regions with tropical and maritime climates. Thornton and Running (1999) improved upon the parameterization of the Bristow–Campbell coefficients, but their model of atmospheric transmittance still underestimates radiation in maritime and tropical regions (Bowling, 1999).

1.3. Objectives

In an effort to find a practical method that will give good estimates of R_s over the earth's land surface, including the tropics, maritime regions, and other humid areas, we developed a model called VP-RAD (for Vapor Pressure Radiation). Like the Bristow–Campbell model, VP-RAD makes its predictions from the limited data set of daily T_{\max} , T_{\min} and $prcp$, along with site latitude, elevation, and mean annual temperature for the parameters. We tested VP-RAD at 17 locations in the United States where we could obtain radiation and climate data for the same time period. After

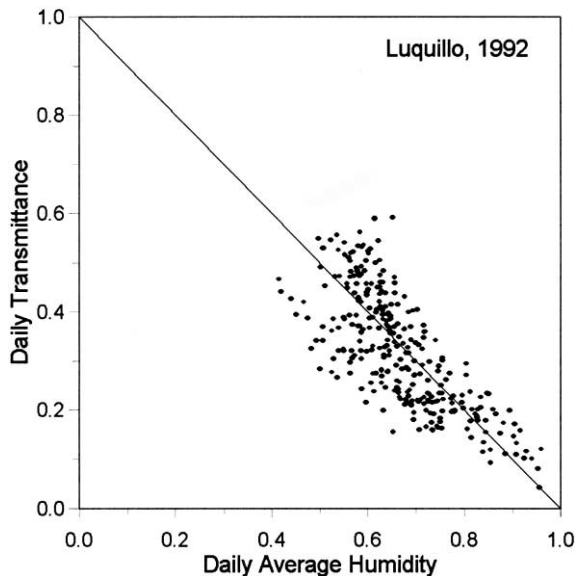


Fig. 1. Observed daily atmospheric transmittance (τ) versus observed daily average humidity (rh_{ave}) at Luquillo, Puerto Rico (Table 1) showing an inverse, nearly linear relationship between τ and rh_{ave} . The solid line is the equation $\tau = 1 - rh_{\text{ave}}$.

establishing that VP-RAD performed well, we compared it to the newest version of MT-CLIM (Thornton et al., 1997), which includes substantial improvements in estimating the coefficients of the Bristow–Campbell equation. Next, we tested VP-RAD globally by comparing its estimates of photosynthetically active radiation to estimates from satellite observations of cloud cover for 1987 (Pinker and Laszlo, 1992). Situations where this model may be used are when R_s data are not available or suspect, when historical temperature records are used to drive ecosystem models, and development of global change scenarios that are not derived from global climate models.

2. VP-RAD model

2.1. Relationship between transmittance and relative humidity

VP-RAD evolved from our observation that there was an inverse, nearly linear relationship between τ and daily average relative humidity (rh_{ave}) at Luquillo, Puerto Rico (Fig. 1). Since relative humidity is seldom measured over large areas, a model relating τ and rh_{ave} would not fulfill our research objectives. Relative humidity is the ratio of the atmospheric vapor pressure to the saturated vapor pressure and can be estimated from daily minimum and maximum temperature (Glassy and Running, 1994; Kimball et al., 1997); therefore, the $\tau \approx 1 - rh_{\text{ave}}$ at a tropical locations had potential. Upon analysis, we concluded that the $\tau \approx 1 - rh_{\text{ave}}$ relationship was not caused by the attenuation of solar radiation by atmospheric water vapor, but rather resulted from the temperature dependence of the saturated vapor pressure for air. Over the course of a typical day, the incoming radiation causes an increase in air temperature, which causes a drop in relative humidity. Therefore, during the rise of air temperature from T_{\min} to T_{\max} , the total radiation received during this time period ($R^{T_{\max}}$) is related to the decline in the instantaneous relative humidity, or $R^{T_{\max}} \propto rh^{T_{\min}} - rh^{T_{\max}}$, where rh^T is the relative humidity at the time of temperature T . In most cases, $rh^{T_{\min}}$ is very close to 1.0 (Bristow and

Campbell, 1984) and the expression can be simplified to $R^{T_{\max}} \propto 1 - rh^{T_{\max}}$. Furthermore, $R^{T_{\max}}$ represents a large portion, but not all, of the total incoming radiation accumulated during the day (R_s). If the function D is defined to represent the ratio $R_s/R^{T_{\max}}$, substitution yields: $R_s \propto D(1 - rh^{T_{\max}})$ for the daylight period.

2.2. Preliminary model relating R_s and relative humidity

To convert the $R_s \propto D(1 - rh^{T_{\max}})$ relationship into a quantitative prediction equation for R_s , we considered three factors. First, since our initial inquiries suggested that a linear relationship between τ and relative humidity could give adequate estimates of R_s at a tropical location like Luquillo, we assumed a linear prediction model. Second, data from other locations suggested that the slope between R_s and $rh^{T_{\max}}$ was not always equal to minus unity, so an additional parameter, β , is required for variation among sites. Third, it had not escaped our notice that the saturation vapor pressure of air is an exponential function of temperature, so the relationship is functionally similar to the Bristow–Campbell equation. It was possible that the R_s relationship offered a method of calculating tropically applicable Bristow–Campbell coefficients from available environmental data (Section 2.3). By design, the quantity $1 - \beta rh^{T_{\max}}$ is meant to reflect the *drop* in relative humidity over the course of the day; consequently, $\beta \geq 0$ and $0 \leq \beta rh^{T_{\max}} \leq 1.0$. The maximum value of R_s cannot exceed $\tau_{\text{cf}}Q_o$, where τ_{cf} is the atmospheric transmittance of the cloud-free atmosphere. Thus, the initial prediction equation is:

$$R_s = \tau_{\text{cf}}D(1 - \beta rh^{T_{\max}})Q_o \quad (3)$$

where the quantity $D(1 - \beta rh^{T_{\max}})$ is limited to a maximum value of 1.0.

Cloud-free atmospheric transmissivity is not a constant value. We estimated τ_{cf} from site latitude, elevation and mean annual temperature. It is divided into three parts:

$$\tau_{\text{cf}} = (\tau_o \tau_a \tau_v)^{P/P_o} \quad (4)$$

where τ_o is the transmittance of clean, dry air, τ_a represents the transmittance affected by atmospheric aerosols and ozone, τ_v is the transmittance affected by atmospheric water vapor, and P/P_o is a correction for site elevation. Following Jones (1992) and Pearcy et al. (1991), at site elevation z (m), the correction factor for elevation is:

$$P/P_o = [1 - (2.2569 \times 10^{-5})z]^{5.2553} \quad (4a)$$

where P is the atmospheric pressure, and P_o is the standard pressure (both in kPa). The latitudinal variation of τ_o can be calculated analytically; however, errors in the formula are introduced at latitudes greater than 60° (Gates, 1980). Instead of using an analytical formula and correcting it for refraction and the earth's curvature, we determined τ_o using linear regression on data from tables 133 and 136 in the Smithsonian Meteorological Tables (List, 1971):

$$\tau_o = 0.947 - (1.033 \times 10^{-5})(|\phi|^{2.22}) \quad (4b)$$

for $|\phi| \leq 80^\circ$ and

$$\tau_o = 0.774 \quad (4c)$$

for $|\phi| > 80^\circ$, where $|\phi|$ is the absolute value of the site latitude. The absorption of radiation by aerosols is extremely variable and inherently unpredictable from our limited data set; therefore, we set τ_a equal to 1.0 for this study. Since warmer areas have more water vapor in the air column, we estimated τ_v as an empirical function:

$$\tau_v = 0.9636 - 9.092 \times 10^{-5}[(T_{\text{mean}} + 30)^{1.8232}] \quad (4d)$$

where T_{mean} is the mean annual temperature ($^\circ\text{C}$). Eq. (4d) was derived by combining a prediction of atmospheric water content as a function of temperature (Showalter, 1945) with an estimate of radiation transmittance loss as a function of water content (Charney, 1945) then applying linear regression to produce a continuous function that estimates transmittance from temperature. These estimates assume a substantial water column that is completely saturated and would apply only at the warmest, most humid sites. Therefore, in most cases, τ_v is equal to 1.

In the model implementation, daily rainfall affects τ_v for convenience. On days when $prcp > 1.0$

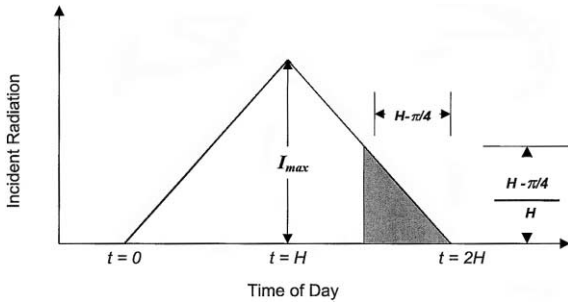


Fig. 2. Illustration of the calculation of function D . To simplify its calculation, we assumed that the instantaneous radiation reaching the earth's surface at time t increased linearly from a sunrise value of zero to a maximum of I_{\max} at noon then decreased linearly to a sunset value of zero. Plotted against time, the incoming radiation would form a triangle with height I_{\max} and a base with a length equal to the day length ($2H$), which varies with the day of the year. R_s is then given by the area of the triangle; $R_s = HI_{\max}$. The quantities $1 - rh_{\text{ave}}$ and $1 - rh^{T_{\max}}$ both typically reach their maximum at around 3 p.m., which, converted to radians ($2\pi/24$ radians h^{-1}) is $t = H + \pi/4$. The total radiation received at the earth's surface from sunrise to 3 p.m. ($R_{3\text{PM}}$) is then R_s minus the area of a triangle with a base of length $H + \pi/4$ and a height $I_{\max}(H + \pi/4)/H$ or $R_{3\text{PM}} = HI_{\max} - 0.5 I_{\max} (H + \pi/4)(H + \pi/4)/H$. Function D is then given by $D = R_s/R_{3\text{PM}}$, which yields $D = [1 - (H - \pi/4)^2/2H^2]^{-1}$.

mm (designated a 'wet' day), the predicted radiation was always greater than the observed. To account for this difference, τ_v was reduced by 0.13 on wet days. This distinction between dry and wet days improved results and is consistent with other models (Bristow and Campbell, 1984; Liu and Scott, 2001).

Function D corrects for errors introduced by site differences in day length. This error arises from the difference between the time of T_{\max} , where the relative humidity reaches its minimum, and sunset where R_s reaches its total daily value. To correct for this difference, we introduced a day length correction $D = R_s/R^{T_{\max}}$. The magnitude of D depends upon the time difference of the maximum values of R_s and $R^{T_{\max}}$, the day length, and the magnitude of the instantaneous radiant flux density. All vary with latitude and time of year. The instantaneous radiant flux density decreases after solar noon. The total incoming radiation, in contrast, continues to accumulate until sunset (Fig. 2). By assuming that the high temperature

(and corresponding minimum in relative humidity) occurs around 3 p.m., the day-length correction is approximated by:

$$D = R_s/R_{T_{\max}} = [1 - (H - \pi/4)^2/2H^2]^{-1} \quad (5)$$

where H is the half-day length (Sellers, 1965).

We tested Eq. (3) using measured relative humidity at seven locations spanning biomes from the boreal forest to tropical rain forests (BOREAS, Jabraas, Pawnee, FIFE, Oak Ridge, Luquillo and Los Diamantes in Table 1). We found that relative humidity was useful in predicting solar irradiance when combined with improved estimates of τ_{ef} , the day-length correction, D , and some adjustment of β .

2.3. VP-RAD model using air temperatures

Saturation vapor pressure (kPa) is estimated as a function of temperature $e_s(T)$ with $e_s(T) = 0.611 \exp[mT/(n + T)]$ where m and n are empirical constants. When $T \geq 0$ °C, m and n have values of 17.269 and 237.7, respectively. For temperatures less than 0 °C, m and n are 21.875 and 265.3, respectively (Bolton, 1980). Relative humidity, vapor pressure, or dewpoint temperature is seldom measured at ground meteorological stations. However, under typical night conditions, T_{\min} is an adequate estimate of the morning dew point temperature (Glassy and Running, 1994; Kimball et al., 1997). This is not true in desert regions, where another method of estimating relative humidity is necessary (Kimball et al., 1997). Since our objective is to improve the prediction of R_s in tropical and maritime areas primarily, we defer improvements on the estimation of dewpoint temperature from T_{\min} for further research (see Section 3.1). Thus, the VP-RAD prediction equation is:

$$R_s = \tau_{\text{ef}} D [1 - \beta e_s(T_{\min})/e_s(T_{\max})] Q_0 \quad (6)$$

where $e_s(T_{\min})$ and $e_s(T_{\max})$ are saturation vapor pressures at T_{\min} and T_{\max} , respectively. The minimum value of R_s is set to be $0.1Q_0$ because, some diffuse radiation inevitably arrives at the earth's surface. From List (1971), table 152), nimbostratus clouds reduce irradiance by about 85%, so a minimum value of $0.1Q_0$ is reasonable.

VP-RAD estimates R_s from a daily input data set consisting of only T_{\max} , T_{\min} , and $prcp$, with mean annual temperature, mean annual tempera-

ture range (see Eq. (9)), site latitude and elevation (z) used for the parameters. Because the VP-RAD model is based upon the relationship between the

Table 1
Model development and evaluation sites

Site	Latitude	Longitude	z (m)	Year	T_{mean} (°C)	T_m (°C)	Annual $prcp$ (m)
<i>Model development sites</i>							
BOREAS ^a	54N	106W	450	1994	1.91	10.17	0.33
Jädraås ^b	60N	20E	185	1987	2.79	10.00 ^j	0.65
Pawnee ^c	41N	105W	1650	1987	8.70	17.20	0.43
FIFE ^d	39N	96W	400	1987	– ^t	– ^t	– ^t
Manhattan ^e	39N	96W	320	1971	12.90	11.86	0.88
Canberra ^f	35S	149E	622	1985	12.92	13.35	0.69
Oak Ridge ^g	36N	84W	305	1993	14.91	11.87	1.02
Luquillo ^h	18N	66W	107	1992	24.45	9.34	2.70
Los Diamantes ⁱ	10N	84W	249	1981	24.46	8.83	5.62
<i>Model evaluation sites</i>							
Bethune ^j	29N	81W	52	1998	21.97	11.58	1.16
Bluefield ^k	37N	81W	803	1999	11.21	13.66	0.83
Canyon ^l	35N	102W	1067	1999	16.10	16.10	0.50
Elizabeth ^m	36N	98W	4	1999	16.15	12.03	1.28
Johnson ⁿ	30N	95W	33	1999	21.20	12.57	1.01
Mississippi Valley ^o	34N	90W	52	1999	21.23	13.72	0.64
Savannah ^p	32N	81W	11	1999	19.25	13.44	1.06
Austin ^q	30N	98W	213	1999	21.87	14.48	0.34
El Paso ^r	32N	106W	1219	1999	18.80	15.26	0.21
Jornada ^s	33N	107W	1360	1999	17.82	15.68	0.19

When data were missing, that day was eliminated from the analysis.

^a Boreal Ecosystem Atmosphere Study Southern Site, Prince Albert National Park, Saskatchewan, Canada (Sellers et al., 1997).

^b Swedish Conifer Experiment, Jädraås, Sweden (Axelsson and Bräkenhielm, 1980).

^c Shortgrass Steppe Long Term Ecological Research Site, USDA Agricultural Research Service Central Plains Experimental Range, Pawnee National Grassland, Colorado, USA.

^d First ISLSCP Field Experiment, Konza Prairie LTER Site, Kansas, USA (Betts and Ball, 1995, 1998).

^e Manhattan Municipal Airport, Manhattan, Kansas, USA.

^f Biology of Forest Growth Experiment, Australian Capital Territory, Australia (Benson et al., 1992).

^g Walker Branch Watershed Throughfall Displacement Experiment, Oak Ridge, Tennessee, USA (Hanson et al., 1998; Wullschleger et al., 1998).

^h Luquillo Experimental Forest Long Term Ecological Research Site, El Verde, Puerto Rico.

ⁱ Los Diamantes, Costa Rica.

^j Bethune-Cookman College, Daytona, Florida, USA.

^k Bluefield, West Virginia, USA.

^l West Texas AM University, Canyon, Texas, USA.

^m Elizabeth City State University, Elizabeth City, North Carolina, USA.

ⁿ Johnson Space Center, Houston, Texas, USA.

^o Mississippi Valley State University, Ita Bena, Mississippi, USA.

^p Savannah State College, Savannah, Georgia, USA.

^q University of Texas-Austin, Austin, Texas, USA.

^r University of Texas-El Paso, El Paso, Texas, USA.

^s Jornada Long Term Ecological Research Site, New Mexico, USA.

^t The FIFE study lasted 5 months; therefore, annual means or totals could not be calculated.

typical daily rise in air temperature and the incoming radiation, errors will be introduced on days when cold or warm air advection causes changes in the daily temperature range. Our limited data set offers no satisfactory way to identify these days, and the averaging of 2 days of temperature data, proposed by Bristow and Campbell (1984) yielded no improvement when applied to this model. Consequently, VP-RAD contains no correction for cold or warm air advection, and enhancements are deferred until further research.

2.4. Using VP-RAD to calculate the Bristow–Campbell coefficients

The VP-RAD equation can be used to calculate the Bristow and Campbell coefficients, since the two models have the same exponential form with air temperature. Bristow–Campbell coefficient A can be deduced by inspection as $A = \tau_{cf} D$. Substituting the exponential expressions for $e_s(T_{\min})$ and $e_s(T_{\max})$ into Eq. (2) yields $A[1 - \exp(-B \cdot \Delta T)]$, where $\Delta T = T_{\max} - T_{\min}$, so $B = -\ln[e_s(T_{\min})/e_s(T_{\max})]/\Delta T$. Setting $\beta \exp(-B \cdot \Delta T)$ equal to $\exp(-B \Delta T^C)$ and solving for C yield $-\ln(\Delta T)[\ln\{\Delta T - [\ln(\beta)/B]\}]$. When these coefficients are used, the Bristow and Campbell equation performs identically to VP-RAD.

2.5. Statistical analyses

The goodness of fit (R^2) between simulated and observed values was determined:

$$R^2 = 1 - \frac{\sum (y_{\text{obs}} - y_{\text{pred}})^2}{\sum (y_{\text{obs}} - y_{\text{mean}})^2} \quad (7)$$

where y_{obs} is the observed value, y_{pred} is the predicted value and y_{mean} is the mean observed value (Mayer and Butler, 1993). The root mean square error (RMSE) was calculated:

$$\text{RMSE} = \left\{ (1/n) \sum (y_{\text{obs}} - y_{\text{pred}})^2 \right\}^{0.5} \quad (8)$$

where n is the number of observations (Mayer and Butler, 1993).

3. VP-RAD model evaluation

3.1. Model development sites

The VP-RAD algorithm was developed from our analyses of meteorological data at seven test sites (Table 1). Some of the sites were selected (Oak Ridge and Canberra) because previous work indicated that the Bristow–Campbell-based MT-CLIM (Running et al., 1987; Glassy and Running, 1994) worked well there, and we wanted to assess the effects of any model changes. Other sites were selected (Pawnee and Luquillo) because MT-CLIM did not work well there. Finally, we used the BOREAS, Manhattan KS, and Los Diamantes sites to test specific hypotheses that arose during model formulation; however, these data were incorporated as test sites for subsequent model development.

At each of the model development sites, 1 year of observed radiation was compared to VP-RAD predictions. We were able to keep coefficient β almost constant with a value near unity (1.041) over a range of sites with differing climates without compromising performance. At locations where β did have to differ substantially from 1.041, primarily mountainous regions with very large daily temperature ranges, we found that we could adequately predict it from

$$\beta = \text{MAX}\{1.041, 23.753 \cdot \Delta T_m / (T_{\text{mean}} + 273.16)\} \quad (9)$$

where ΔT_m is the mean annual temperature range between T_{\max} and T_{\min} (Fig. 3).

At all of the sites, when T_{\min} exceeded 20 °C, VP-RAD performed better setting $T_{\min} = 20$ °C. Below 20 °C, the slope of saturated vapor pressure with respect to temperature is low so that the error in using $e_s(T_{\min})$ in place of $e_s(T_d)$ is small (Glassy and Running, 1994), whereas above 20 °C, the slope is large, and the approximation of T_d with T_{\min} is poor. Alternatively, in areas with very high dew points, the daily temperature range is small, and the correlation between incoming radiation and temperature rise breaks down.

The R^2 values for observations compared to predictions of daily irradiance from VP-RAD were greater than 0.66 for the temperate and

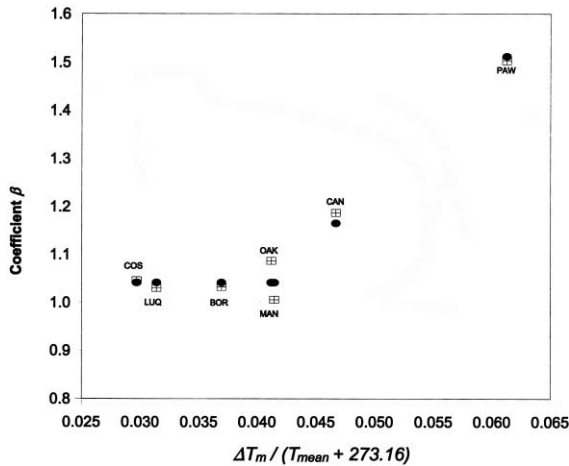


Fig. 3. VP-RAD coefficient β for the developmental test sites as a function of the mean annual difference between maximum and minimum temperature expressed as a fraction of the mean annual temperature. The black dots represent the predicted values. The crossed squares indicate the coefficient value determined from the best overall fit to the data. Abbreviations are: BOREAS site (BOR), Pawnee (PAW), Canberra (CAN), Manhattan (MAN), Oak Ridge (OAK), Luquillo (LUQ), and Los Diamantes (COS).

boreal sites (Table 2). At Luquillo and Los Diamantes, performance was overall lower (R^2 values of 0.49 and 0.56, respectively). Predicted and observed radiation scattered around the one-to-one line except for Luquillo (Fig. 4). Unlike the Britstow–Campbell-based models mentioned previously, VP-RAD showed no tendency generally to over- or underestimate in any of the biomes; errors in the mean annual R_s were always within $0.6 \text{ MJ m}^{-2} \text{ day}^{-1}$ (Table 3; Fig. 5).

3.2. Model evaluation sites

We located 10 additional sites where a year of daily radiation was measured and nearby weather data were available. Seven of these sites (Bethune, Bluefield, Elizabeth, Johnson, Mississippi Valley, Savannah, and Austin) were in moist humid areas, one (Canyon) was in a marginal-to-dry area, and two (El Paso, Jornada) were in semi-arid areas. None of these sites were used to develop or calculate any of the VP-RAD coefficients. We used these locations to check our model formulation by comparing the measured radiation to the VP-RAD estimates (Table 2).

Table 2

Model results of VP-RAD for development and evaluation sites

Site	R^2	RMSE ^a	Pred. ^b	Error ^c
<i>Model development sites</i>				
BOREAS	0.81	3.49	11.40	−0.10
Pawnee	0.69	4.26	14.98	−0.08
Manhattan	0.73	4.41	15.69	−0.48
Canberra	0.76	3.81	15.58	+0.28
Oak Ridge	0.91	2.46	14.35	+0.49
Luquillo	0.49	3.64	11.28	−0.17
Los Diamantes	0.56	2.87	11.02	+0.08
<i>Model evaluation sites (warm, humid)</i>				
Bethune	0.51	4.62	16.49	−0.77
Bluefield	0.42	5.88	15.95	+0.70
Elizabeth	0.65	4.26	14.72	−0.28
Johnson	0.62	3.85	16.96	+0.19
Mississippi Valley	0.75	3.51	18.22	+0.07
Savannah	0.76	3.42	16.34	−0.41
Austin	0.63	4.20	17.24	+0.54
<i>Model evaluation sites (semi-arid)</i>				
Canyon	0.55	4.34	16.15	−0.63
El Paso	0.39	5.23	17.01	−3.69
Jornada	0.54	4.55	16.88	−3.23

^a Root mean square error.

^b Predicted average daily solar irradiance ($\text{MJ m}^{-2} \text{ day}^{-1}$) for the year.

^c Difference between observed and predicted average daily solar irradiance ($\text{MJ m}^{-2} \text{ day}^{-1}$).

Table 3

MT-CLIM 4.3 (Thornton and Running, 1999) statistics for warm, humid model-evaluation sites in the USA for comparison with VP-RAD statistics in Table 2

	R^2	RMSE ^a	Pred. ^b	Error ^c
Bethune	0.39	5.15	14.21	−3.02
Bluefield	0.18	7.12	18.18	3.16
Elizabeth City	0.43	5.63	17.52	−2.07
Johnson	0.53	4.42	15.03	−1.52
Savannah	0.68	3.91	14.91	−2.73
Mississippi Valley	0.66	4.07	16.05	−2.10
Austin	0.56	4.68	15.76	−0.79

^a Root mean square error.

^b Predicted average daily solar irradiance ($\text{MJ m}^{-2} \text{ day}^{-1}$) for the year.

^c Difference between observed and predicted average daily solar irradiance ($\text{MJ m}^{-2} \text{ day}^{-1}$).

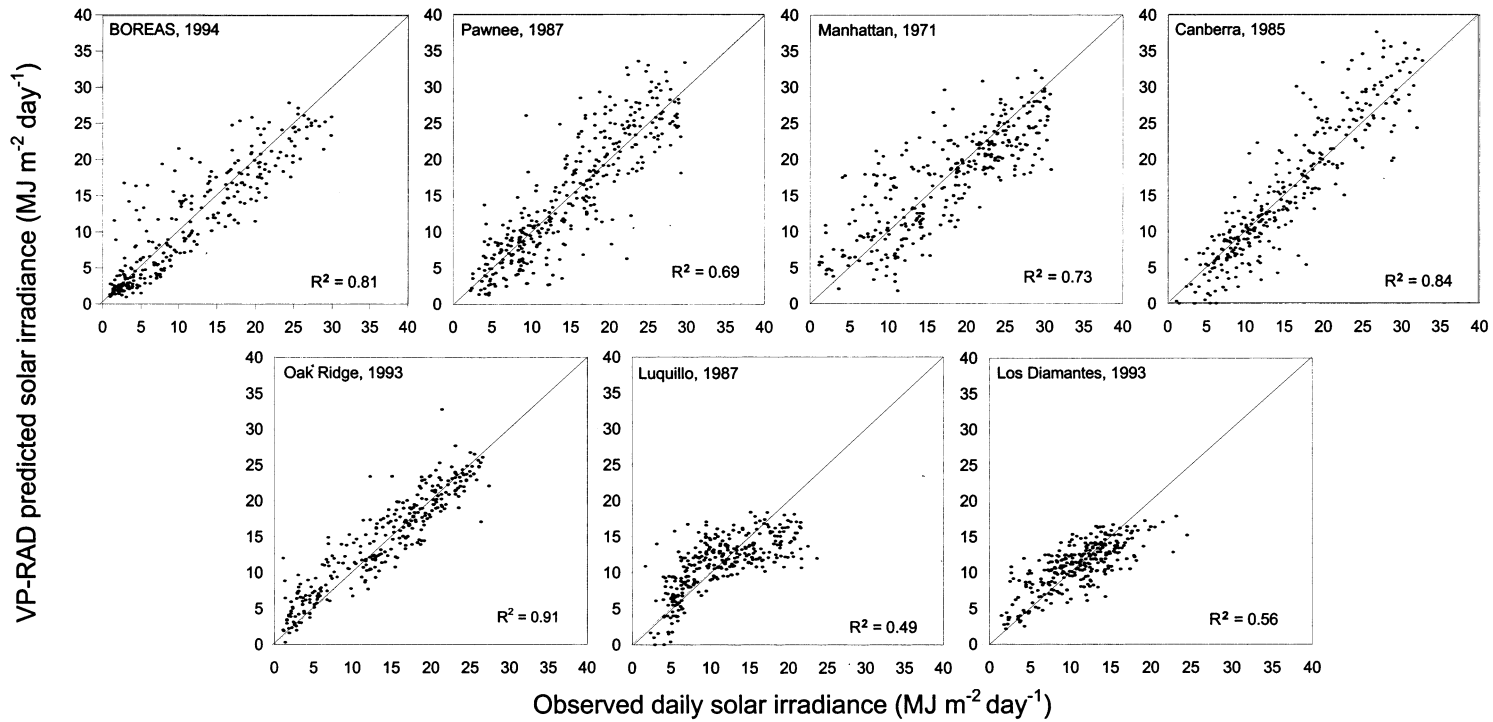


Fig. 4. VP-RAD predicted R_s versus the observed daily radiation at the model development sites in Tables 1 and 2.

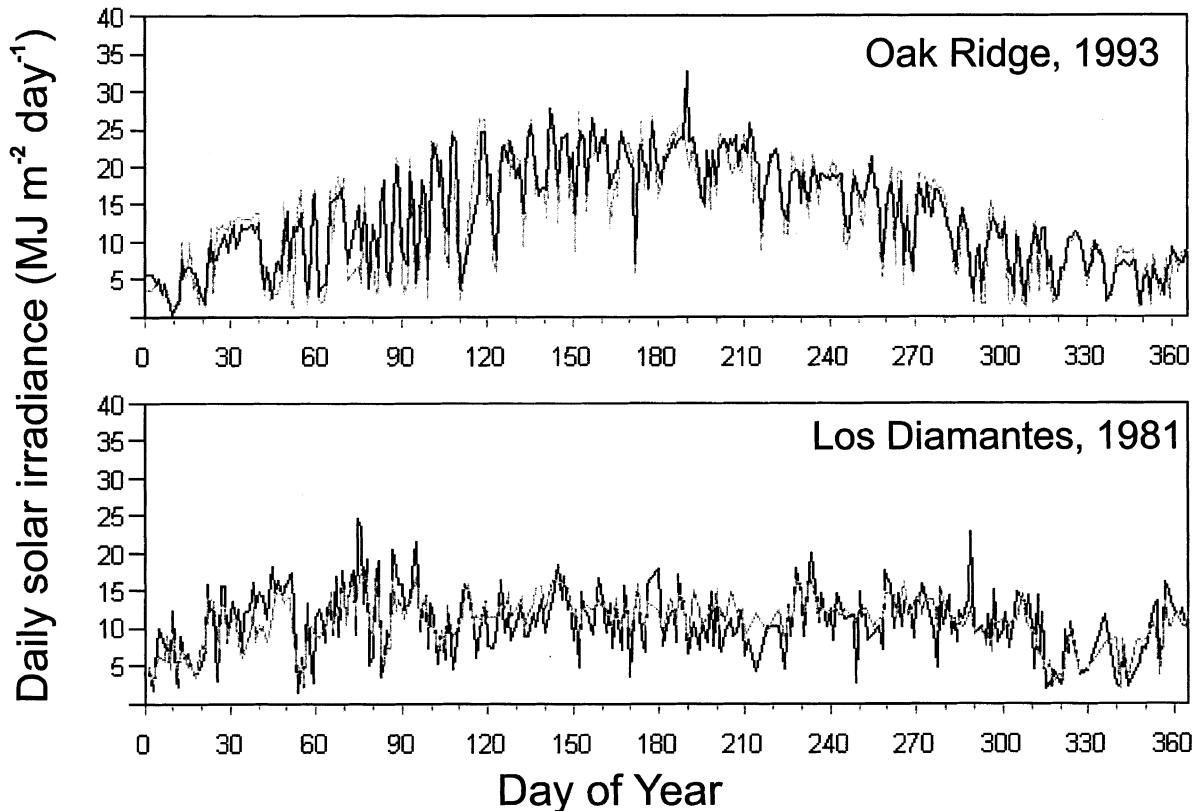


Fig. 5. Day-to-day variation of VP-RAD predicted radiation for Oak Ridge, Tennessee, and Los Diamantes, Costa Rica. The heavy line is the observed daily solar irradiance (R_s), and the thin line is the VP-RAD predicted R_s .

The R^2 values and the mean absolute error of annual R_s were similar to the developmental test sites (Table 2). As expected, performance was poor at the two desert locations (El Paso and Jornada), where VP-RAD underestimated the total radiation that had arrived, because T_d is much lower than T_{min} . The predictions of R_s at these desert sites were considerably improved when we lowered T_{min} to be closer to the actual dew point temperatures. At El Paso, approximating actual T_d improved the R^2 values from 0.39 to 0.71 and improved RMSE from -3.69 to 0.12 $\text{MJ m}^{-2} \text{ day}^{-1}$. At Jornada, the R^2 values improved from 0.54 to 0.69, and the RMSE fell from -3.23 to -1.06 $\text{MJ m}^{-2} \text{ day}^{-1}$. These improvements suggest that VP-RAD should be improved for desert conditions by using a better method of estimating the dew point temperature.

3.3. Comparison with MT-CLIM

Since our research objective was to develop a model that gave improved performance in the moist, humid areas, we compared VP-RAD (Table 2) and MT-CLIM (Table 3) at the seven warm, humid model evaluation sites. At these sites, an older version of MT-CLIM substantially underestimated R_s , so the results in Table 3 show that the latest version, MT-CLIM 4.3 (Thornton and Running, 1999), is an improvement compared to the older version. However, this comparison showed that VP-RAD offered still more improvement in predictions of R_s (Tables 2 and 3).

3.4. Global evaluation

Evaluation of a point model like VP-RAD over a large-area grid is problematic. To be computa-

tionally manageable and true to the actual availability of environmental data, global analyses often take place on a grid of about 1° of latitude by 1° of longitude, or larger. Each grid cell, which in the tropics is about 100 km square, is assumed to have the same environmental characteristics. On a day-to-day basis, this is clearly not true; cloud cover and temperature can vary substantially over 100 km. The main problem, however, is the total lack of any radiation measurements over large, remote areas. Therefore, we compared VP-RAD predictions to those of a model driven by satellite observations of cloud cover (Pinker and Laszlo, 1992; Pinker et al., 1995). The Pinker and Laszlo model estimates photosynthetically active radiation (PAR, $\text{MJ m}^{-2} \text{day}^{-1}$ for wavelengths from 0.4 to 0.7 μm) using a different algorithm that has been independently validated. Therefore, comparison between them should be useful to highlight areas where one model or the other may need improvement.

Since the original Pinker and Laszlo satellite-derived PAR are on a $2.5 \times 2.5^\circ$ grid, they were regridded to $1 \times 1^\circ$ while conserving the areal monthly average of PAR (Hunt et al., 1996). R_s was predicted using VP-RAD for the year 1987 over the earth's non-barren land area (Matthews, 1983) and converted into PAR by assuming that PAR is 50% of R_s (Szeicz, 1974; Stanhill and Fuchs, 1977; Howell et al., 1983; Rao, 1984). Gridded temperature and precipitation data for 1987 were from Piper and Stewart (1996). These climate data are interpolated on a $1 \times 1^\circ$ grid from surface meteorological observations and consist of daily maximum and minimum temperature and daily total precipitation. ETOPO5 elevation data were regridded, weighted by areal extent, to 1° grid cells by Hunt et al. (1996) for calculation of τ_{cr} . The global distribution of 1987 annual average daily PAR estimated by VP-RAD (annual total PAR divided by 365 days) is shown in Fig. 6. The absolute differences between annual-average daily VP-RAD PAR and satellite-derived PAR are shown in Fig. 7. Because seasonal biases may be hidden in annual totals, we also compared average daily PAR for the months of January and July, 1987 (Figs. 8 and 9, respectively).

For 13,072 grid cells examined, VP-RAD derived PAR and satellite-derived PAR converged to within $\pm 1.0 \text{ MJ m}^{-2} \text{day}^{-1}$ over 72% of the earth's non-barren land surface and agreed to within $\pm 2.0 \text{ MJ m}^{-2} \text{day}^{-1}$ over 91% of the land surface. VP-RAD predictions were slightly lower by approximately $2\text{--}3 \text{ MJ m}^{-2} \text{day}^{-1}$ compared to satellite-derived PAR in Central America and Brazil, Central Africa, parts of Australia and, to a lesser extent, in the extreme northern coastal areas of North America and Eurasia (Fig. 7). A smaller area reflecting the same magnitude of lower prediction is also present in Southeast Asia. Larger differences (about $4 \text{ MJ m}^{-2} \text{day}^{-1}$) occur in North and Eastern Australia and Indonesia (Fig. 7). The monthly comparisons indicated greater divergence in these areas during the dry season (Fig. 8) than in the wet season (Fig. 9).

Long-term radiation climatologies (Landsberg, 1961; United States Department of Commerce, 1964; Berliand, 1970; World Meteorological Organization, 1981) suggest that satellite-derived PAR estimates may be slightly high in these areas. The climatologies show a region of relatively high average PAR ($\approx 9\text{--}10 \text{ MJ m}^{-2} \text{day}^{-1}$) in South America extending over the northern part of Chile into northwest Argentina and Paraguay. To the north and east is a relative low ($\approx 7\text{--}8 \text{ MJ m}^{-2} \text{day}^{-1}$) extending across most of the Amazon basin. VP-RAD predicted these magnitudes and also picked up the difference between the two regions (Fig. 6), but the satellite-derived PAR was similar ($\approx 9\text{--}10 \text{ MJ m}^{-2} \text{day}^{-1}$). In the Congo Basin, the VP-RAD predictions also agreed well with the climatologies by predicting a relative low of about $6\text{--}8 \text{ MJ m}^{-2} \text{day}^{-1}$ surrounded to the north, east and south by a relative high of about $9\text{--}10 \text{ MJ m}^{-2} \text{day}^{-1}$ (Fig. 6). In another tropical region, Southeast Asia, the VP-RAD predictions agreed with the climatologies. Although satellite-derived PAR picked up these patterns, the estimated values were approximately $2 \text{ MJ m}^{-2} \text{day}^{-1}$ higher than the climatological averages.

A comparison of 1987 observed annual average radiation in the Democratic Republic of the Congo, Philippines, Malaysia, and Australia (Table 4) confirmed that VP-RAD estimates were generally appropriate for these areas, and the

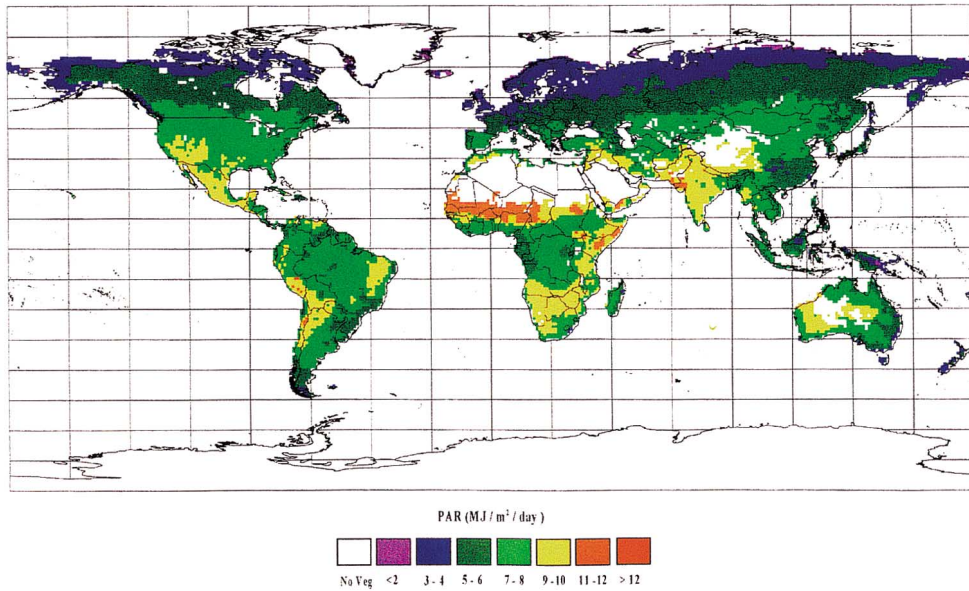


Fig. 6

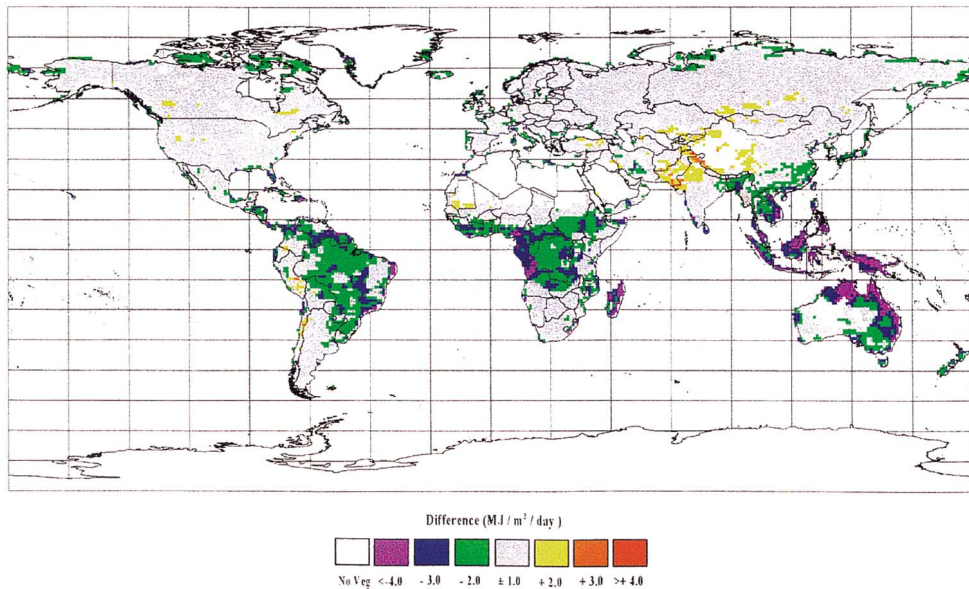


Fig. 7

Fig. 6. Annual-average PAR ($\text{MJ m}^{-2} \text{ day}^{-1}$) for the year 1987 predicted by the VP-RAD model using the Piper and Stewart (1996) global climate data set. White areas indicate where the PAR was not calculated, because the terrestrial grid cell was considered barren, and thus climate data were not gridded.

Fig. 7. Difference of annual-average PAR for 1987 predicted by VP-RAD and the Pinker and Laszlo satellite-derived PAR. Results are shown as VP-RAD PAR minus satellite-derived PAR and expressed in $\text{MJ m}^{-2} \text{ day}^{-1}$. Gray areas indicate where VP-RAD and satellite-derived PAR converged to within $\pm 1.0 \text{ MJ m}^{-2} \text{ day}^{-1}$; areas shown in white were not calculated.

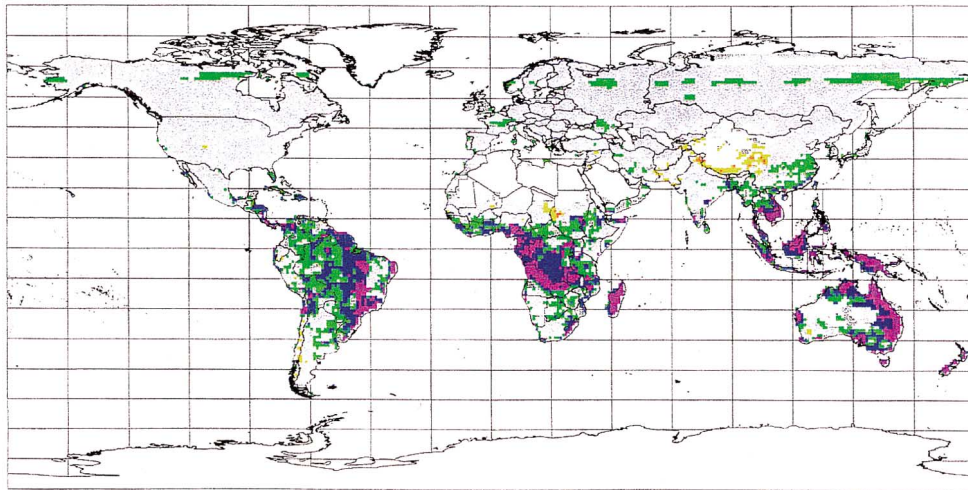


Fig. 8

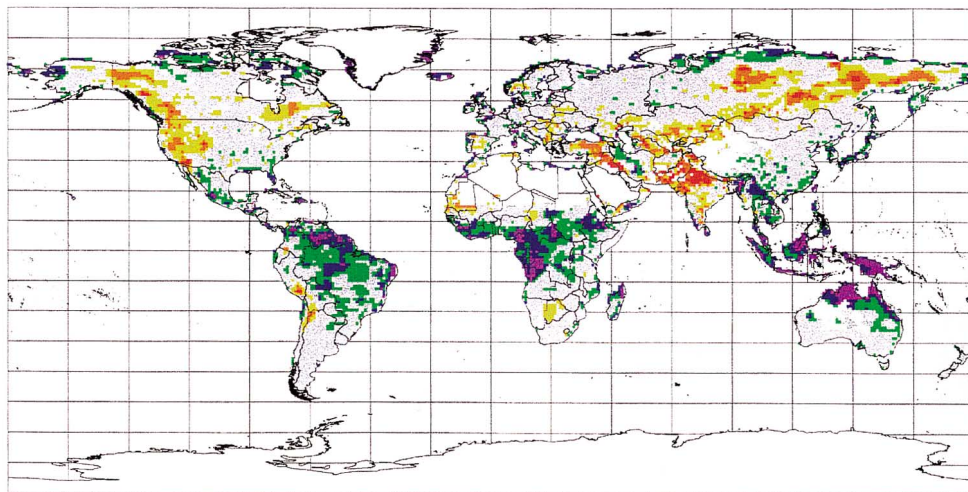


Fig. 9

Fig. 8. Difference of monthly-average PAR for January 1987, predicted by VP-RAD and the Pinker and Laszlo satellite-derived PAR. White and gray areas are defined in Fig. 7.

Fig. 9. Difference of monthly-average PAR for July 1987, predicted by VP-RAD and the Pinker and Laszlo satellite-derived PAR. White and gray areas are defined in Fig. 7.

satellite-derived PAR was slightly high, as suggested by the climatologies. Examination of the January and July totals also confirmed this. How-

ever, in Northern and Eastern Australia, VP-RAD was consistently low, whereas the satellite-derived PAR was slightly high. Therefore,

in this region, differences between satellite-derived PAR and VP-RAD predictions are a combination of low predictions by VP-RAD and slightly high satellite-derived PAR estimates. Both sites in Australia are on the coast and lie within an area where Piper and Stewart (1996) noted that the precipitation frequency was overestimated because of poor weather station density. Therefore, it is possible that τ_v was low because of the applied daily precipitation correction in these areas, thereby resulting in a low prediction of PAR by VP-RAD.

Table 4

Average PAR ($\text{MJ m}^{-2} \text{ day}^{-1}$) at selected points from observed climatologies and modelled PAR for 1987 from VP-RAD and satellite observations of cloud cover

Site (latitude, longitude)			
Period	Observed	VP-RAD	Satellite
<i>Kinshasha, Democratic Republic of the Congo (4.4S, 15.3E)</i>			
Annual	7.3	7.5	10.5
January	7.4	7.5	9.5
July	5.5	5.5	9.5
<i>Kananga, Democratic Republic of the Congo (5.9S, 22.4E)</i>			
Annual	8.1	7.5	9.5
January	7.2	5.5	9.5
July	6.8	7.5	11.5
<i>Science Garden, Philippines (14.6N, 121.0E)</i>			
Annual	7.9	7.5	9.5
January	7.1	7.5	7.5
July	6.5	7.5	9.5
<i>Kuala Lumpur, Malaysia (3.1N, 101.6E)</i>			
Annual	8.0	7.5	11.5
January	7.0	5.5	7.5
July	8.0	7.5	11.5
<i>Brisbane, Australia (27.4S, 153.1E)</i>			
Annual	8.7	7.5	11.5
January	11.3	7.5	11.5
July	6.2	3.5	5.5
<i>Darwin, Australia (12.5S, 130.8E)</i>			
Annual	9.5	7.5	11.5
January	7.7	7.5	11.5
July	9.3	5.5	9.5

Data from the World Radiation Data Centre (WRDC). The WRDC is maintained for the World Meteorological Organization by the Russian Federal Service for Hydrometeorology and Environmental Monitoring, A.I. Voeikov Main Geophysical Observatory, St. Petersburg, Russia and is available on the website <http://wrdc-mgo.nrel.gov/>.

Further inland, the under-prediction may arise from the majority of the weather stations of those 1° -latitude-by- 1° -longitude grid cells being on the coast where the moderating effects of the nearby oceans cause the daily temperature range to be generally smaller than in the grid-cell interior. A similar situation is true for Central America, where we could not find 1987 observations (Piper and Stewart, 1996).

VP-RAD produces higher predictions of PAR in mountainous areas than satellite-derived PAR; differences are obvious for the July monthly totals in western North America and in Himalayan mountains (Fig. 9) but not as noticeable in the annual totals (Fig. 7) and January monthly totals (Fig. 8). The satellite-derived PAR does not include elevation in its calculation of PAR (Pinker and Laszlo, 1992). However, the Piper and Stewart (1996) values are usually interpolated from surrounding, low elevation, stations, and errors in the estimated lapse rates for T_{\min} and T_{\max} could have resulted in values of estimated ΔT that are higher than actual (Running et al., 1987; Glassy and Running, 1994). Therefore, VP-RAD predictions of PAR may be too high. We conclude that the differences between satellite-derived PAR and VP-RAD predictions in mountainous regions are a combination of slightly high predictions by VP-RAD and slightly low satellite-derived PAR estimates.

4. Conclusions

VP-RAD is a model developed from an observed relationship between daily total atmospheric transmittance and daily average relative humidity. The relationship is not based on the direct reduction of τ by water vapor but rather on the rise in air temperature (and decrease in relative humidity) caused by incoming radiation that is attenuated by clouds. VP-RAD works with the limited data set of daily precipitation, minimum air temperature and maximum air temperature, which are readily available for sites around the world. The coefficients of VP-RAD can be converted into the coefficients of the Bristow–Campbell equation (Eq. (2)), which has been used for local-, regional- and global-scale applications. Therefore, VP-RAD offers a conve-

nient method for dynamically calculating site-specific coefficients, instead of tuning the coefficients with long-term climatological data.

The general convergence between VP-RAD and satellite-derived PAR ($\pm 1.0 \text{ MJ m}^{-2} \text{ day}^{-1}$ for 72% of 13,072 independent validations) shows that the model is globally applicable, with some problems unresolved for coastal areas. However, compared to the previous global calculations of daily irradiance (Hunt et al., 1996) using an older version of MT-CLIM, VP-RAD did substantially better in these regions, and these improvements will affect predicted global carbon and water fluxes.

VP-RAD can be incorporated into models such as MT-CLIM and RHESSys for the spatial and temporal resolution necessary to drive models of hydrologic and biogeochemical processes. Furthermore, MT-CLIM and RHESSys were applied to various global climatic change studies, such as the VEMAP project (Kittel et al., 1995), and VP-RAD could be used for these simulations, if care is taken in warm, moist locales, to provide improved estimates of the incoming solar radiation under the changed temperature and precipitation regimes. Finally, the VP-RAD model will be useful for estimating irradiances from long-term records of daily climate where either historical records of solar radiation data may be biased due to infrequent sensor calibration or radiation data may be simply unavailable.

Acknowledgements

Special thanks to Sharon Stewart for assistance with the computer graphics. We are also grateful to the many people who provided us with the climatic data necessary to develop and test our models: Ingrid C. Burke, William K. Lauenroth and Chris Wasser at the Shortgrass Steppe LTER site; Paul J. Hansen at Oak Ridge National Laboratory; Shuguang Liu and William A. Reiners for data from Los Diamantes, Costa Rica; Richard L. Vanderlip at Manhattan, Kansas; Alan K. Betts for the FIFE data; the staff at the Luquillo Experimental Forest LTER site; and Robert D. Kelly, Jeff A. Newcomer and David R. Landis for BOREAS data; the CONFRRM website ([\[redc.nrel.gov/solar/confrrm\]\(http://redc.nrel.gov/solar/confrrm\)\) for radiation data from Bethune, Bluefield, Elizabeth, Johnson, Savannah, Mississippi Valley, Canyon, El Paso and Austin; the NSF LTER website for radiation and weather data for Jornada; the World Radiation Data Centre \(WRDC\) for radiation data from Kinshasha, Kananga, Science Garden, Kuala Lumpur, Darwin, and Brisbane. We especially thank C. David Keeling, Peter E. Thornton, William K. Smith, Robert D. Kelly, Steven T. Jackson, Jeff M. Welker, Shuguang Liu, Richard L. Vanderlip, Dennis D. Baldocchi, and Ted M. Zobeck for their helpful comments. This research was completed with funding from: \(1\) The National Institute for Global Environmental Change, Southeast Regional Center at the University of Alabama; \(2\) NASA grants NAG5-3861 and NAG-3528; and \(3\) a University of Wyoming Space Grant Planetary and Space Science Center Graduate Fellowship to J.C. Winslow.](http://</p>
</div>
<div data-bbox=)

References

- Antonić, O., 1998. Modelling daily topographic solar radiation without site-specific hourly radiation data. *Ecol. Model.* 113, 31–40.
- Axelsson, B., Bråkenhielm, S., 1980. Investigation sites of the Swedish Coniferous Forest Project—biological and physiographical features. In: Persson, T. (Ed.), *Structure and Function of Northern Coniferous Forest—An Ecosystem Study*, Ecological Bulletins, Stockholm, vol. 32, pp. 25–64.
- Benson, M.L., Landsberg, J.J., Borough, C.J., 1992. The biology of forest growth experiment: an introduction. *For. Ecol. Manage.* 52, 1–16.
- Berliand, T.G., 1970. *Solar Radiation and Radiation Balance Data (The World Network)*. Hydrometeorological Publishing House, Leningrad 598 pp.
- Betts, A.K., Ball, J.H., 1995. The FIFE surface diurnal cycle climate. *J. Geophys. Res.* 100, 25679–25693.
- Betts, A.K., Ball, J.H., 1998. FIFE surface climate and site-average dataset 1987–1989. *J. Atm. Sci.* 55, 1091–1108.
- Bolton, D., 1980. The computation of equivalent potential temperature. *Mon. Weath. Rev.* 108, 1046–1053.
- Bowling, L., 1999. Technical Note: Solar Radiation, The Variable Infiltration Capacity (VIC) Macroscale Hydrologic Model Home Page (http://www.hydro.washington.edu/Lettenmaier/Models/VIC/Technical_Notes/Notes_radiation.html). University of Washington.
- Bristow, K.L., Campbell, G.S., 1984. On the relationship between incoming solar radiation and daily maximum and minimum temperature. *Agric. For. Meteorol.* 31, 159–166.

- Charney, J., 1945. Radiation. In: Berry, F.A., Bolla, E., Beers, N.R. (Eds.), *Handbook of Meteorology*, first ed. McGraw-Hill, New York, pp. 284–311.
- Friend, A.D., 1998. Parameterisation of a global daily weather generator for terrestrial ecosystem modelling. *Ecol. Model.* 109, 121–140.
- Gates, D.M., 1980. *Biophysical Ecology*. Springer, New York 611 pp.
- Glassy, J.M., Running, S.W., 1994. Validating diurnal climatology logic of the MT-CLIM model across a climatic gradient in Oregon. *Ecol. Appl.* 4, 248–257.
- Gu, J., Smith, E.A., 1997. High-resolution estimates of total solar and PAR surface fluxes over large-scale BOREAS study area from GOES measurements. *J. Geophys. Res.* 102, 29685–29705.
- Hanson, P.J., Todd, D.E., Huston, M.A., Joslin, J.D., Croker, J., Augé, R.M., 1998. Description and Field Performance of the Walker Branch Throughfall Displacement Experiment: 1993–1996. ORNL/TM_13586. Oak Ridge National Laboratory, Oak Ridge, TN 47 pp.
- Howell, T.A., Meek, D.W., Hatfield, J.L., 1983. Relationship of photosynthetically active radiation to shortwave radiation in the San Joaquin Valley. *Agric. Meteorol.* 28, 157–175.
- Hunt, E.R. Jr., Martin, F.C., Running, S.W., 1991. Simulating the effects of climatic variation on stem carbon accumulation of a ponderosa pine stand: comparison with annual growth increment data. *Tree Physiol.* 9, 161–171.
- Hunt, E.R. Jr., Piper, S.C., Nemani, R.R., Keeling, C.D., Otto, R.D., Running, S.W., 1996. Global net carbon exchange and intra-annual atmospheric CO₂ concentrations predicted by an ecosystem process model and three-dimensional atmospheric transport model. *Glob. Biogeochem. Cycles* 10, 431–456.
- Jones, H.G., 1992. *Plants and Microclimate*. Cambridge University Press, Cambridge 428 pp.
- Kimball, J.S., Running, S.W., Nemani, R., 1997. An improved method for estimating surface humidity from daily minimum temperature. *Agric. For. Meteorol.* 85, 87–98.
- Kittel, T.G.F., Rosenbloom, N.A., Painter, T.H., Schimel, D.S., Modelling Participants, V.E.M.A.P., 1995. The VEMAP integrated database for modelling United States ecosystem/vegetation sensitivity to climate change. *J. Biogeogr.* 22, 857–862.
- Landsberg, H.E., 1961. Solar Radiation at the earth's surface. *Solar Energy* 5, 95–98.
- List, R.J., 1971. *Smithsonian Meteorological Tables*, sixth ed. Smithsonian Institution Press, Washington, DC 527 pp.
- Liu, D.L., Scott, B.J., 2001. Estimation of solar radiation in Australia from rainfall and temperature observations. *Agric. For. Meteorol.* 106, 41–59.
- Matthews, E., 1983. Global vegetation and land use: new high-resolution data bases for climate studies. *J. Clim. Appl. Meteorol.* 22, 474–487.
- Mayer, D.G., Butler, D.G., 1993. Statistical Validation. *Ecol. Model.* 68, 21–32.
- Nikolov, N.T., Zeller, K.F., 1992. A solar radiation algorithm for ecosystem dynamic models. *Ecol. Model.* 61, 149–168.
- Piper, S.C., Stewart, E.F., 1996. A gridded global data set of daily temperature and precipitation for terrestrial biospheric modeling. *Glob. Biogeochem. Cycles* 10, 757–782.
- Pearcy, R.W., Ehleringer, J.R., Mooney, H.A., Rundel, P.W., 1991. *Plant Physiological Ecology: Field Methods and Instrumentation*. Chapman & Hall, New York 455 pp.
- Pinker, R.T., Laszlo, I., 1992. Modeling surface solar irradiance for satellite applications on a global scale. *J. Appl. Meteorol.* 31, 194–211.
- Pinker, R.T., Laszlo, I., Whitlock, C.H., Charlock, T.P., 1995. Radiative flux opens a new window on climate research. *Eos, Trans. Am. Geophys. Union* 76, 145, 155, 158.
- Rao, C.R.N., 1984. Photosynthetically active components of global solar radiation: measurements and model computations. *Arch. Meteorol. Geophys. Bioclim.*, B 34, 353–362.
- Running, S.W., Nemani, R.R., Hungerford, R.D., 1987. Extrapolation of synoptic meteorological data in mountainous terrain and its use for simulating forest evapotranspiration and photosynthesis. *Can. J. For. Res.* 17, 472–483.
- Running, S.W., Nemani, R.R., Peterson, D.L., Band, L.E., Potts, D.F., Pierce, L.L., Spanner, M.A., 1989. Mapping regional forest evapotranspiration and photosynthesis by coupling satellite data with ecosystem simulation. *Ecology* 70, 1090–1101.
- Sellers, P.J., Hall, F.G., Kelly, R.D., Black, A., Baldocchi, D., Berry, J., Ryan, M., Ranson, K.J., Crill, P.M., Lettenmaier, D.P., Margolis, H., Cihlar, J., Newcomer, J., Fitzjarrald, D., Jarvis, P.G., Gower, S.T., Halliwell, D., Williams, D., Goodison, B., Wickland, D.E., Guertin, F.E., 1997. BOREAS in 1997: Experiment overview, scientific results, and future directions. *J. Geophys. Res.* 102, 28731–28769.
- Sellers, W.D., 1965. *Physical Climatology*. The University of Chicago Press, Chicago, IL 272 pp.
- Showalter, A.K., 1945. Quantitative determination of maximum rainfall. In: Berry, F.A., Bolla, E., Beers, N.R. (Eds.), *Chapter in Handbook of Meteorology*, first ed. McGraw-Hill, New York, pp. 1015–1027.
- Stanhill, G., Fuchs, M., 1977. The relative flux density of photosynthetically active radiation. *J. Appl. Ecol.* 14, 317–322.
- Szeicz, G., 1974. Solar radiation for plant growth. *J. Appl. Ecol.* 11, 617–636.
- Thornton, P.E., Running, S.W., White, M.A., 1997. Generating surfaces of daily meteorological variables over large regions of complex terrain. *J. Hydrol.* 190, 214–251.
- Thornton, P.E., Running, S.W., 1999. An improved algorithm for estimating incident daily solar radiation from measurements of temperature, humidity and precipitation. *Agric. For. Meteorol.* 93, 211–228.
- United States Department of Commerce, 1964. *Mean Daily Solar Radiation, Monthly and Annual*. US Government Printing Office, Washington, DC.

World Meteorological Organization, 1981. Meteorological Aspects of the Utilization of Solar Radiation as an Energy Source. Technical Note No. 172. WMO Publication No. 557. Secretariat of the World Meteorological Organization, Geneva 298 pp.

Wullschleger, S.D., Hanson, P.J., Tschaplinski, T.J., 1998.

Whole-plant water flux in understory red maple exposed to altered precipitation regimes. *Tree Physiol.* 18, 71–79.

Yin, X., 1996. Reconstructing monthly global solar radiation from air temperature and precipitation records: a general algorithm for Canada. *Ecol. Model.* 88, 38–44.